Common clock GNSS-baselines at PTB

J. Leute, A. Bauch
Physikalisch-Technische Bundesanstalt, Bundesallee 100, 38116 Braunschweig, Germany

S. Schön, T. Krawinkel
Institut für Erdmessung
Leibniz Universität Hannover, Schneiderberg 50, D-30167 Hannover, Germany

Abstract. The experiments presented in this paper represent to some extent the merger of the disciplines that are abbreviated as Positioning, Navigation and Timing (PNT). They had been proposed in the context of the EMRP project "Surveying" with the hope that the different communities may learn from each other. A varying group of GNSS receivers has been operated at the campus of Physikalisch-Technische Bundesanstalt (PTB) during the last three years on different buildings, connected to the same hydrogen maser as a highly stable frequency reference. This network has been used as test-bed for the study of distance and distance variation determinations with the common-clock single-difference approach. Data from common-clock experiments on zero, short, and very short baselines with different receivers are presented. Focus is laid on the impact of temperature variations in the receivers and cables, and on the impact of asymmetries in measurement set-ups. The implementation of the underlying so-called common-clock configuration is discussed in some detail.

Keywords. GNSS- based distance measurement, GNSS-based time and frequency comparisons, time and frequency metrology, atomic clocks

1 Introduction

The reception and processing of signals from global satellite navigation systems (GNSS) have become a standard procedure in the disciplines geodesy, distance measurements for deformation monitoring, time and frequency metrology, not to mention the abundant use in hand-held devices, including smart-phones. Signal processing strategies in the various disciplines are quite different. In many positioning and geodetic applications, double-differences are formed to reduce distance dependent systematic effects and to eliminate the receiver and satellites' clock biases. In time comparisons, however, the difference between two clocks connected to two remotely operated receivers is the measurement quantity of interest, and in this application the signal delays in the individual receivers as well as biases (and their variations) introduced due to signal routing at the installations have to be dealt with.
Several GNSS receivers, some of which had been provided by Institut für Erdmessung (IfE), Leibniz-University Hannover, have been operated at the campus of Physikalisch-Technische Bundesanstalt (PTB) during the last three years on different buildings, some almost continuously, others on occasion of special campaigns. They have been connected to the same highly stable frequency reference, signals representing the local reference time scale UTC(PTB) that is derived from a steered active hydrogen maser. In the following section we briefly discuss the quality of this frequency reference and its dissemination on the campus. This receiver network has been used as testbed for the study of distance and distance variation determinations with the common-clock single-difference approach (Santerre and Beutler (1993)). Data from common-clock experiments on zero, very short, and short baselines with different receivers are presented in sections 3 to 5. Focus is laid on the impact of temperature variations in the receivers and cables, and on the impact of asymmetries in measurement set-ups. This paper yields a more detailed description of some observations reported previously (Schön et al. (2016)) where it was shown that the concept of common-clock single-differences is not the first choice for the determination of static differences but may have other applications when the focus is on high resolution distance variations, especially in the vertical component.

JISDM 2016 Vienna

2 Installations at PTB

2.1 Realization of UTC(PTB)

Time and frequency signals involved in the studies reported here are derived from PTB's local realization of Coordinated Universal Time, named UTC(PTB). Since February 2010 UTC(PTB) has been realized using an active hydrogen maser as signal source whose frequency is steered via a commercial high resolution offset generator (Bauch et al. (2012)). Steering is based on day-to-day basis on the comparison between the maser involved and PTB's primary fountain clocks CSF1 and CSF2. In the long term, UTC(PTB) is steered towards UTC based on the data published in the BIPM Circular T. Between July 2010 and end 2015 the maximum absolute rate of UTC-UTC(PTB) during any standard 5-day interval was 0.44 ns/d, and the time difference never exceeded 10 ns. UTC(PTB) signals exist in the form of 1 pulse-per-second (1PPS) and standard frequency signals (5 MHz, 10 MHz, and 100 MHz). The relative frequency instability is about 1×10^{-13} at one second averaging, $1x10^{-15}$ at 10^4 s. UTC(PTB) serves as the basis for all of PTB's time services and international time comparisons.

2.2 Replica of UTC(PTB) at a remote location

The UTC(PTB) signal is primarily generated at Kopfermann building which houses PTB's atomic clocks and most time transfer equipment. It is transmitted to a second laboratory located in the Meitner building via modulating an optical carrier with 100 MHz representing UTC(PTB) frequency and generating a 1 PPS signal on site.

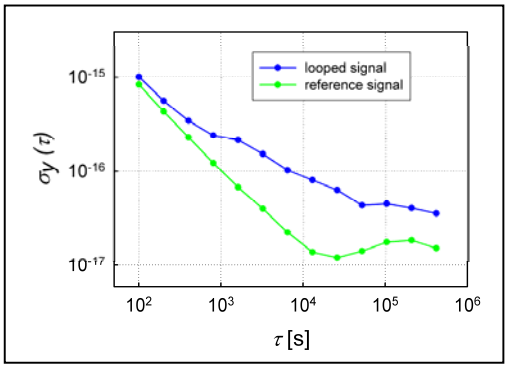

Fig. 1. Relative frequency instability of 100 MHz UTC)PTB) signals employed in the study.

For monitoring purposes the 100 MHz-signal is transmitted back to Kopfermann building and its phase is compared with the original generated signal. This loop thus encompasses about 1.4 km of fibre, two modulators and two demodulators, and a 100 MHz distribution amplifier. Conversion of phase to relative frequency differences allows an instability analysis to be made. The result is shown in Figure 1 for the looped-back signal with reference to the transmitted signal (blue trace), and for a second output of the 100 MHz signal source with respect to the transmitted signal (green trace). The latter measurement practically defines the noise floor of the measurement. A slight degradation at averaging times longer than 1000 s is obvious for the loop-back channel. However, the signal quality was initially considered as good enough for starting the baseline experiments.

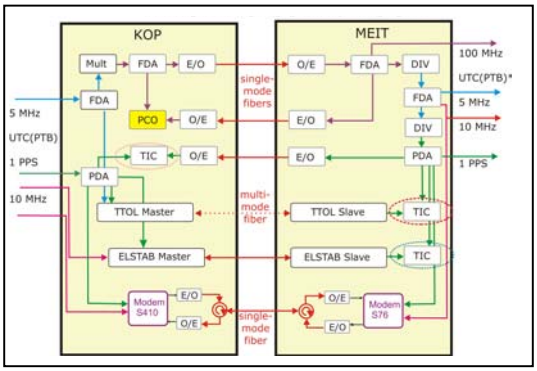

Fig.2. Transfer and monitoring of UTC(PTB)* generated in Meitner building (MEIT) (FCA, PDA: frequency and pulse distribution amplifiers, DIV: divider, TIC: time interval counter, E/O electric to optical signal converter, TTOL and ELSTAB are explained in the text.

The 1 PPS signal generated at Meitner building is currently offset by about 136 ns from UTC(PTB), but this offset is continuously monitored with up to three independent installations that are depicted in Figure 2. Here the yellow "PCO" represents the measurement system described above. Monitoring of 1 PPS differences is based on two commercial fiber-based time transfer systems, TTOL (for Time Transfer via Optical Link), manufactured by TimeTech GmbH Stuttgart, and ELSTAB (for Electronically Stabilized Time and Frequency Distribution Over Optical Fiber, Sliwczyński et al. (2013)), and signal exchange between two modems usually employed in Two-way satellite time transfer (TW), here connected through a single-mode fiber (Rost et al. (2012)). Each of the systems had been individually calibrated with uncertainties well below

1 ns. Figure 3 gives evidence that the three methods have agreed almost at the 0.1 ns level at least for some weeks.

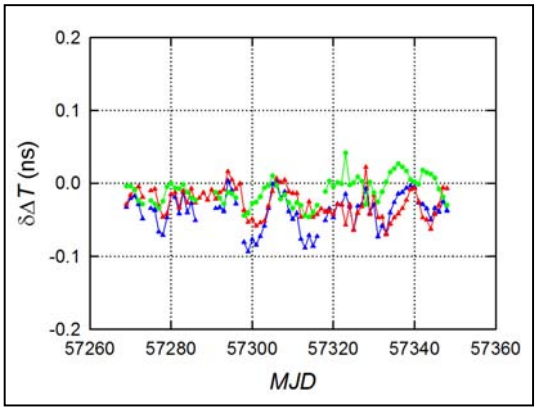

Fig. 3. Monitoring of 1 PPS differences between UTC(PTB) and UTC(PTB)*, double differences AGH-TW (blue), TTOL-TW (red) and TTOL-AGH (green) (see Figure 2) during about 80 days. MJD 57360 correspond to 2015-12-04.

2.3 GNSS receiving equipment in PTB

Fig. 4. Upper: Aerial view of the two PTB buildings and antenna sites initially involved, lower: antenna pillars (from left to right) MEI1, MEI4, MEI3 (both populated) and MEI2.

GNSS receiving equipment comprises the antenna, the antenna cable, the receiver and the local connection to 1 PPS and 10 MHz signals. Initially, antennae were installed on pillars MEI1 and MEI2 on the Meitner building, which are free of obstructions down to 0° elevation angle as they are located above the trees/forest at the PTB campus. MEI1 and MEI2 are of equal height and separated by approximately 5 m. Later pillars MEI3 to MEI7 were constructed that have superior mechanical stability – although the mechanical properties of MEI1 and MEI2 were never identified as causing problems.

A set of fixed antenna posts exists on the roof of the Kopfermann building, one of which, KOP1 was used in the current study. It is located a few meters away from the site of the IGS station PTBB, approximately 16 m below and 290 m away from MEI1. This site is far from ideal as the near forest, yields obstructions up to elevations of 25°. Figures 4 and 5 show the station environment.

Fig. 5. Close-up: Antenna post KOP1 with the antenna used during the studies discussed in Section 5; background: PTBB (IGS) and PTBG antennas.

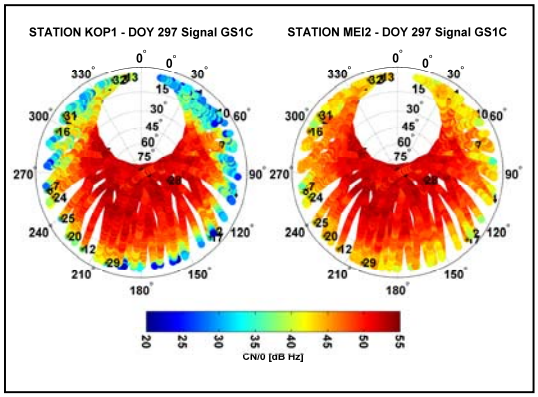

Fig. 6. Skyplots with color-coded carrier to noise density ratios, from observations at KOP1 (left) and MEI1 (right), respectively. A common color scale is applied. Bluish colors indicates weak signals.

In Figure 6 so-called sky plots are reproduced that illustrate the quality of the received GPS signals in terms of the carrier to noise density for each satellite for DOY 297 in 2013. The comparison shows the reduced signal strength (bluish colors) at low elevation angles for KOP1, induced by signal diffraction and partial obstructions by trees and foliage.

3 Early very short baseline studies

Zero baseline and very short baseline experiments were initially conducted using pillars MEI1 and MEI2. State-of-the-art geodetic GNSS receiving equipment was utilized, comprising of two Leica choke ring antennas with radome (Leica AR25.R3 LEIT) – absolutely calibrated at IfE –, two JAVAD Delta TRE-G3T and two Leica GRX1200+GNSS receivers. Later one antenna and two receivers were moved to the Kopfermann building (antenna post KOP1). The scheme is depicted in Figure7.

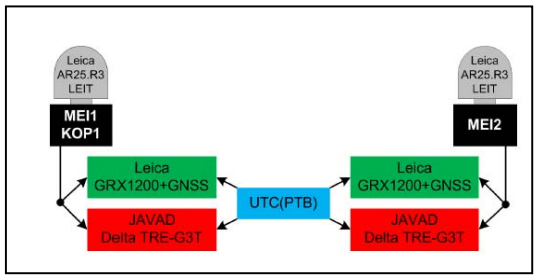

Fig. 7. Measurement set-up in 2013 common-clock experiments.

Each antenna was connected to one JAVAD and one Leica receiver via active signal splitters. The signal delays of the long antenna cables (ca. 20 m – 60 m) between antenna and splitter were calibrated by PTB before the measurement campaign, therefore, the corresponding values (ca. 120 ns – 240 ns) were in principle known with an uncertainty of less than 1 ns. In the context of this study such delays are of particular relevance if they are subject to variations with time caused by temperature variations. For the selected antenna cable type, Andrews FSJ-1, the manufacturer reports a quite low delay change as a function of temperature, with a turning point around 20°C. Based on the specifications on can estimate the effect by assuming a slope of around 5 PPM/K around 0°C. Thus one would expect a change of an antenna cable delay of 200 ns of only 1 ps/K.

As an example of the results obtained with the set-up shown in Figure 7, the results of one of the first measurement campaigns is presented in Figure 8 as it already shows part of the issues observed in general.

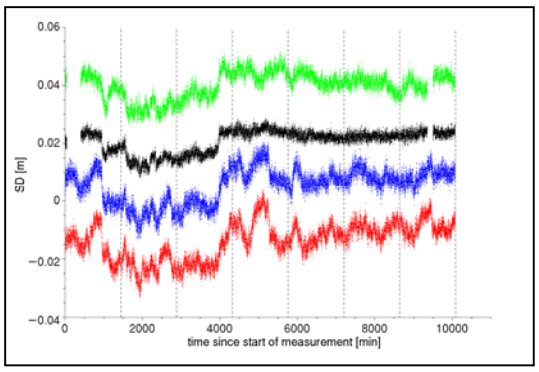

Fig. 8. Very short baseline results (one week) obtained with the two pairs of receivers connected to the posts MEI1 and MEI2 (see Fig. 7), details in the text; vertical lines indicate day boundaries.

In Figure 8 the between-receiver single differences (SD) for the GPS L1 carrier frequency are depicted which were computed based on the respective observed-minus-computed time series of all visible GPS satellites. The previously determined station coordinates were held fixed. A cut-off angle of 5° for the zero and very short baseline and of 30° for the short baseline was selected. An integer ambiguity was subtracted from each satellite track. As the last step, epoch-wise, the weighted (by sine of the satellite elevation) mean value of the single differences was computed. The 4 traces represent the differences between the two Javad (black) and the two Leica (blue) receiver, and mixed links. Common features in all links (e. g. at minute 4000) point to a disturbance in one antenna+cable+ splitter set-up. The red and blue traces share one Leica receiver at post MEI2, and this instrument showed excessive noise also at other sites and in other installations. The offsets between the traces are caused by the phase offsets between the reference signals connected to the receivers due to different length of cables involved – and unknown internal signal delays in the receivers.

4 Example study on a zero baseline

Another set of experiments represented a step back to an even simpler configuration, illustrated in Figure 9. Four JAVAD Delta TRE-G3T receivers were connected to a Leica AR25.R4 LEIT antenna, but connected pairwise to different frequency signals. Short low-loss cables of (nominally) equal length were employed aiming at a symmetric installation. The main purpose was the assessment of the impact of the much higher frequency instability of a rubidium atomic frequency standard (RAFS) ($\approx 4\times10^{-12}$ at τ = 100 s) compared to signals of UTC(Meit) ($\approx 5\times10^{-15}$ at τ = 100 s) under otherwise optimal conditions. It was also investigated whether the usual frequency offset from nominal (a few parts in 10^{10}) of a RAFS has an impact. To this end its frequency was temporarily slaved with a long time constant using a 1 PPS output of a commercial GPS time receiver as steering reference so that the offset became close to zero. No significant effect of the frequency offset could be detected.

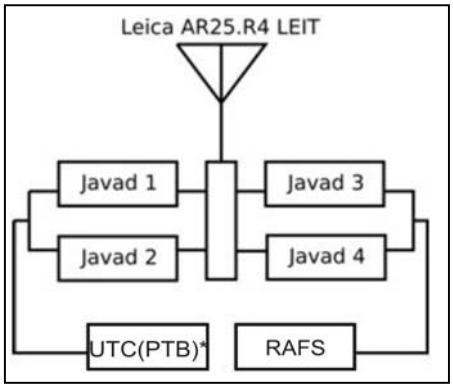

Fig. 9. Zero baseline common clock setup

The evaluated single-differences SD for the two pairs J1-J2 and J3-J4 are shown in Figure 10 for one selected day out of a longer recording series. There is no distinct difference in SD amplitude noted. Both plots reveal a correlation with the temperature of the laboratory despite of the great care to implement a symmetric set-up. The temperature variations were caused by a maladjusted setting of the control parameters of the air-conditioning system in the room that was later cured.

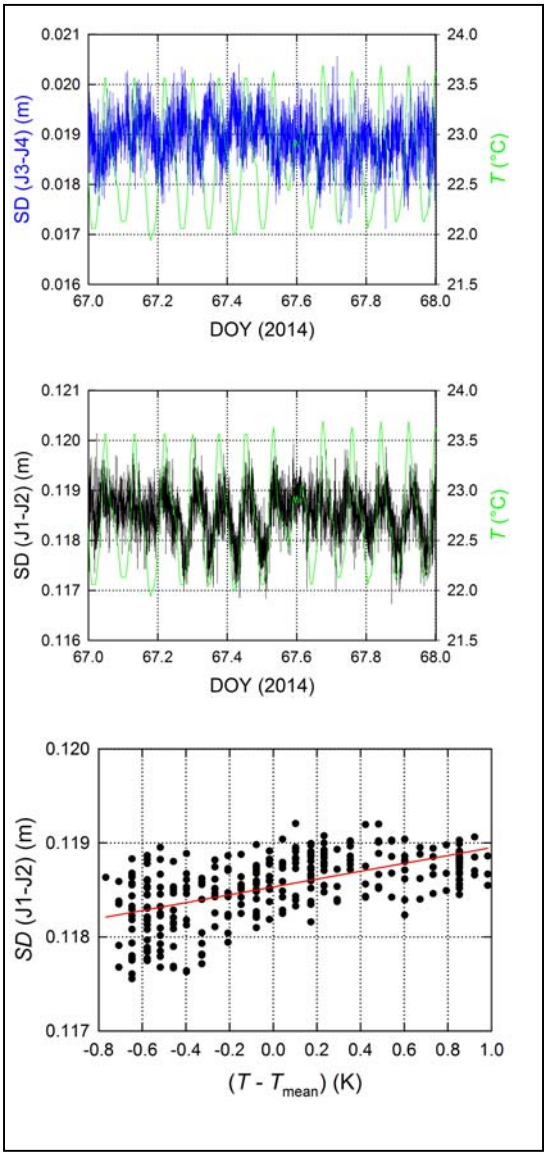

Fig. 10. Single differences between pairs of receivers (Figure 9), J3-J4 (upper). J1-J2 (middle), observed on day 67 of 2014 (2014-03-08), in correlation with temperature in the room of receiver installation; correlation plot (lower), regression lope = (0.418 ± 0.036) mm/K.

A quantitative analysis shows that the sensitivity of SD on temperature variations is between 0.3 mm/K and 0.6 mm/K. From this it should get clear which high degree of symmetry would be needed in a set-up intended for a real surveying task, with receivers located in different environment and long cables subjected to environmental influences (see e.g. Sleewagen et al. (2015)).

If the SD values reported in Figure 10 are corrected for the apparent linear temperature dependence, the residuals have a standard deviation from the mean of 0.32 mm only, a quite remarkable result.

5 Example study on the short baseline

Based on previous experience, a new permanent setup was installed in late 2014, a short baseline of approx. 300 m between the Meitner (MEI3) and the Kopfermann (KOP1) building, and a very short baseline between posts MEI3 and MEI4 (see Figure 4). Efforts were undertaken to reduce the impact of environmental conditions on the measurements. More stable monuments for the antennas were built and modifications on the air-condition system were made that reduced the temperature variations in the Meitner building laboratory. Receivers and antennae involved are listed in Table 1.

Table 1. Instrumentation of recent link studies

Antenna pillar	Receiver	Antenna and radome
MEI3	PolaRx4TR	LEIAR25.R4 LEIT
MEI4	PolaRx4TR	LEIAR20 LEIM
KOP1	PolaRx4TR	NOV750.R4 NOVS

Table 2. Cartesian coordinates in ITRF2008 for the three antenna posts involved

Antenna pillart	(X-3840000)/m	(Y-709000)/m	(Z-5023000)/m
MEI3	3995.138	940.840	159.988
MEI4	3994.294	940.429	160.691
KOP1	4057.206	663.765	131.521

Pillar MEI4 is occupied by the antenna of a Galileo experimental sensor station (GESS), run by GMV as contractor of the Time and Geodetic Validation Facility (TGVF) of Galileo. Antenna cables connecting to MEI3 and MEI4 are both of type FSJ-1 and about 25 m in length. To reach KOP1, a 55 m cable is needed. Here Ecoflex 15plus was used that is more convenient to roll out but has otherwise similar properties. Subsequently we report on some findings for the KOP1 to MEI3 and MEI4 links. Note that the receivers were linked to UTC(PTB) realizations as depicted in Figure 2.

As for previous studies, the antenna coordinates were determined from some days of observations using the NRCan PPP software package (Kouba and Heroux 2001). The coordinates are reported in Table 2. The final coordinates are reached only after several hours of observation, and the delayed availability of the IGS products causes a delay in the processing. This is why other measurement strategies are in general more suitable for actual surveying tasks.

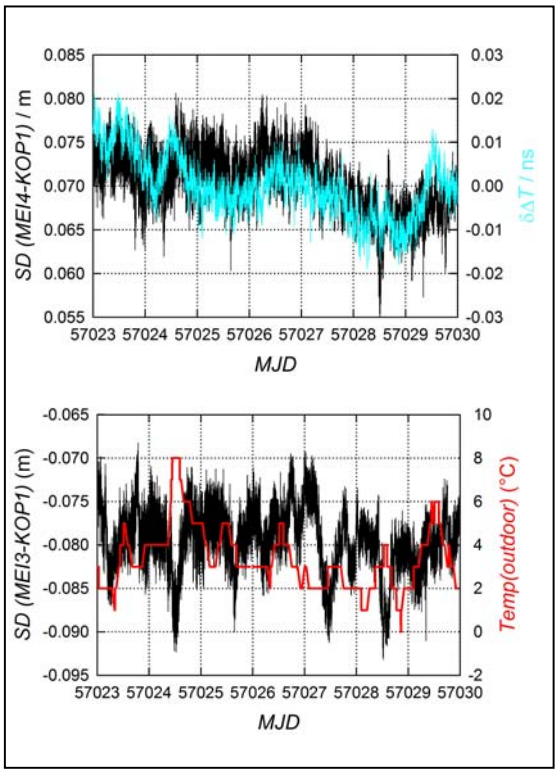

Fig.11. Single differences between pairs of receivers, connected to antennas on posts, MEI4/KOP1 (upper), and MEI3/KOP1 (lower), observed on days 1-7 of 2015, MJD 57023-57029. Second plots: Time difference between the 1 PPS signals connected to the two receivers minus mean value, (transfer via Optical Link) (cyan), outdoor temperature (red).

The determination of single-differences SD followed the steps laid down in Section 3. In Figure 11 the results of the KOP1 – MEI baselines are depicted, and differences in the behaviour of the two nominally identical receivers in a highly

symmetrical installation is obvious. Some of the differences are likely due to the receiver attached to MEI3, but not to the installation at KOP1. In the upper plot the time differences measured with the TIC attached to the TTOL (see Figure 2) are overlaid. So a part of the noted SD variations can be attributed to the non-ideal common-clock condition. In the lower plot the outdoor temperature, measured with a commercial weather station attached to the PTBB IGS station is overlaid. Except for day 57024 there seems no correlation at short time scales to exist. In the long term, the unstabilized fiber transfer of UTC(PTB) will of course be affected by slow temperature variations of the cable in its conduct.

6 Conclusion

In the context of the EMRP project "Surveying" GNSS observations with different sets of receivers and antennae were made which were analyzed using single differences. Even short distance measurements on the PTB campus showed, however, that several sources of disturbances exist that usually cancel in the analysis based on double differences. Two state-of-the art GNSS receivers of the same type in the same rack were shown to exhibit different sensitivity to ambient temperature or humidity variations, exceeding the low picosecond range with time. Thus, common-clock experiments unfortunately proved of little benefit for the investigation of second order uncertainty contributions for determining static distances. One has to note that the assumptions underlying the predictions made by Santerre and Beutler (1993) could not be fulfilled in our installations – and will be hardly fulfilled in general in an installation that comprises distributed equipment. Recently however, Schön et al. (2016) showed that common-clock set-ups could be beneficial for kinematic analyses of distances changes between the GPS stations linked to a common clock. In addition, common-clock set-ups are valuable and adequate test set-ups to investigate and compare the receiver performance of different manufacturers as well as to study various receiver related biases, see e.g. MacLeod et al. (2015).

Acknowledgement

The EMRP is jointly funded by the EMRP participating countries within EURAMET and the European Union. The authors thank Egle Staliuniene, Jürgen Becker, and Thomas Polewka (PTB) for technical support in operation of the GNSS receivers and data handling, and Przemysław Krehlik and Łukasz Śliwczyński from AGH University of Science and Technology, Krakow, Poland, for the loan of the ELSATB system and the fruitful cooperation.

References

Bauch, A., Weyers, S., Piester, D., Staliuniene, E., Yang, W. (2012). Generation of UTC(PTB) as a fountain-clock based time scale. In: *Metrologia,* 49, pp. 180-188.

Kouba, J. and Héroux, P. (2001). Precise point positioning using IGS orbit and clock products. In: *GPS Solutions,* 5, pp. 12-2.

MacLeod, K., Elson, S., Banville, S. (2015), GNSS receiver test site at NRCan, http://www.biasws2015.unibe.ch/presentations.html

Rost, M., Piester, D., Yang, W., Feldmann, T., Wübbena, T. and Bauch, A. (2012). Time transfer through optical fibers over a distance of 73 km with an uncertainty below 100 ps. In: *Metrologia,* 49, pp. 772–778.

Santerre, R. and G. Beutler (1993). A proposed GPS method with multi-antennae and single receiver. In: *Bulletin Géodésique*, 67, pp. 210–223.

Schön, S., Hue Pham, K., Kersten, T., Leute, J., and Bauch, A. (2016). Potential of GPS Common Clock Single-differences for Deformation Monitoring. In: *Proc. of JISDM 2016,* in preparation.

Sleewagen, J.-M. (2015). Code inter-frequency biases in GNSS receivers, http://www.biasws2015.unibe.ch/presentations.html.

Sliwczyński, Ł., Krehlik, P. Czubla, A., Buczek, Ł. and Lipiński, M. (2013) Dissemination of time and RF frequency via a stabilized fibre optic link over a distance of 420 km, *Metrologia,* 50, pp. 133–145.